

# *In Situ* Fast Transient Fluorescence Technique (FTRF) to Study Swelling of Gels Made of Various Crosslinker Contents

M. Erdoğan, Ö. Pekcan

Department of Physics, Istanbul Technical University, Maslak, Istanbul 80626, Turkey

Received 4 September 2001; accepted 10 February 2002

**ABSTRACT:** The fast transient fluorescence technique (FTRF), which uses the strobe master system (SMS), was employed to study the swelling of disc-shaped PMMA [poly(methyl methacrylate)] gels. Seven gels were prepared by free radical copolymerization (FCC) of methyl methacrylate (MMA) with various ethylene glycol dimethacrylate (EGDM) contents. Pyrene ( $P_y$ ) was introduced as a fluorescence probe during polymerization. After drying these gels, swelling experiments were performed in chloroform at room temperature.  $P_y$  lifetimes were measured from fluorescence decay traces during the *in situ* swelling experi-

ments. An equation was derived for low quenching efficiencies to interpret the behavior of lifetimes in the gel during swelling. It was observed that  $P_y$  lifetimes in the gel decreased as swelling proceeded. The Li–Tanaka equation was used to determine the cooperative diffusion coefficients,  $D_{cr}$ , which were found to decrease as the crosslinker content was increased. © 2002 Wiley Periodicals, Inc. *J Appl Polym Sci* 87: 464–472, 2003

**Key words:** swelling; crosslinker content; gel; time-resolved fluorescence

## INTRODUCTION

Swelling is directly related to the viscoelastic properties of a gel. Gel elasticity and friction between network and solvent play an important role in the kinetics of gel swelling.<sup>1–3</sup> It is known that the relaxation time of swelling is proportional to the square of the linear size of a gel,<sup>1</sup> which has been confirmed experimentally.<sup>3</sup> One of the most important features of the gel-swelling process is that it is isotropic, that is, when the radius increases 10%, the axial length increases 10% in a long cylindrical gel. The elastic and swelling properties of permanent networks can be understood by considering two opposing effects, osmotic pressure and restraining force. Usually the total free energy of a chemically crosslinked network can be separated into two terms: the bulk and the shear energies. In a swollen network the characteristic quantity of the bulk free energy is the osmotic bulk modulus,  $K$ . The other important energy, the shear energy, keeps the gel in shape by minimizing the nonisotropic deformation. The characteristic coefficient of these forces is the shear modulus,  $\mu$ , which can be evaluated most directly by stress–strain measurements.<sup>4,5</sup> Li and Tanaka<sup>6</sup> have developed a model in which shear modulus plays an important role in keeping the gel in

shape because of the coupling of any change in different directions. This model predicts that the geometry of a gel is an important factor and that swelling is not a pure diffusion process.

Fluorescence dyes can be used to study local environments, basically with two types of experiments. When a dye simply is added to the system as a small molecule, the dye is referred to as a probe, which is available commercially. As a consequence, such experiments are easy to carry out but often difficult to interpret because it is necessary to know the location of the dye in the system. If an experiment can be prepared that allows the dyes to be attached covalently to a specific component of a system, such as a polymer chain segment, such dyes are called labels. The question can be raised: does the presence of the dye perturb the system or does it perturb its own local environments in the system? Perturbations are most common when high dye concentration leads to aggregation and in crystalline systems where the order in the system can be affected by the dye. Perturbations are much less likely when fluorescent dye is incorporated into an amorphous fluid or glassy phase. For about two decades the transient fluorescence (TRF) technique for measuring fluorescence decay has been routinely applied to study many polymeric systems, using dyes both as probes and/or as labels.<sup>7–10</sup> TRF spectroscopy with direct energy transfer (DET) and quenching methods has been used to characterize the internal morphologies of composite polymeric materials.<sup>7–11</sup> Film formation from donor- and acceptor-

Correspondence to: Ö. Pekcan (pekcan@itu.edu.tr).

labeled latex particles was studied using DET in conjunction with TRF.<sup>12,13</sup> A single-photon counting (SPC) technique, which produces decay curves and measures lifetimes in conjunction with DET, was used to study the diffusion of small dye molecules within the interphase domain of anthracene and/or phenanthrene-labeled PMMA [poly(methyl methacrylate)] particles.<sup>14,15</sup>

Many experimental techniques have been used to study the kinetics of the swelling and shrinking of chemical and physical gels, among which are quasi-elastic light scattering,<sup>16</sup> neutron scattering,<sup>17</sup> and *in situ* interferometric<sup>18</sup> measurements. Pyrene derivate was used as a fluorescence molecule to monitor the polymerization, aging, and drying of aluminosilicate gels.<sup>19</sup> *In situ* observation of the sol-gel phase transition in free-radical crosslinking copolymerization (FCC) was studied using the steady-state fluorescence (SSF) technique.<sup>20,21</sup> The same technique was also used to study the swelling and drying kinetics in disc-shaped gels.<sup>22</sup> Recently, the fast transient fluorescence technique was employed to model the swelling of PMMA gel in chloroform, in which fluorescence decay profiles were fitted to double exponential function.<sup>23</sup> In these experiments the lifetimes of pyrene ( $\tau_1$  and  $\tau_2$ ), which are related to the inside and outside of the disc-shaped gel, were measured. It was observed that  $\tau_2$  increased as the swelling time was increased; however,  $\tau_1$  remained unchanged during the swelling process. The  $\tau_2$  values were used to determine the swelling parameters, such as the cooperative diffusion coefficient,  $D_c$ , and the time constant,  $\tau$ .

In this work the swelling of disc-shaped gels formed by FCC of MMA with various EGDM contents was studied using the strobe master system (SMS). Fluorescence decay profiles of  $P_y$  were measured when the gel in the fluorescence cell was illuminated directly by the exciting light. SMS was used for lifetime measurements of  $P_y$  in and out of the gel simultaneously. Decay profiles were fitted to the double exponential law to obtain  $\tau_1$  and  $\tau_2$  lifetimes of  $P_y$ . Lifetime measurements with SMS are much more rapid than those done with single-photon counting system and phase instruments. This advantage of SMS allowed us to make at least tens of life measurements during the swelling process of the gels. That is the reason we named this technique fast transient fluorescence (FTRF), as it gives us many advantages compared with other lifetime measuring techniques. It was observed that as the gel became swollen, the lifetime of  $P_y$  in the gel ( $\tau_2$ ) decreased, which was modeled using low quenching and the Stern-Volmer equation. Cooperative diffusion coefficients,  $D_c$ , were determined by employing the Li-Tanaka equation.

## THEORETICAL CONSIDERATIONS

### Kinetics of swelling

It has been suggested<sup>6</sup> that the kinetics of swelling and shrinking of a polymer network or gel should obey the following relationship,

$$\frac{W(t_s)}{W(\infty)} = 1 - \sum_{n=1}^{\infty} B_n e^{-t_s/\tau_n} \quad (1)$$

where  $W(t_s)$  and  $W(\infty)$  are the swelling or solvent uptakes at time  $t_s$  and at infinite equilibrium, respectively.  $W(t_s)$  can also be considered as a volume difference of the gel at time  $t$  and 0. Each component of the displacement vector of a point in the network from its final equilibrium location after the gel is fully swollen decays exponentially with a time constant,  $\tau_n$ , which is independent of time  $t$ . Here  $B_n$  is given by the following relationship<sup>6</sup>

$$B_n = \frac{2(3 - 4R)}{\alpha_n^2 - (4R - 1)(3 - 4R)} \quad (2)$$

where  $R$  is defined as the ratio of the shear and the longitudinal osmotic modulus,  $R = G/M$ . The longitudinal osmotic modulus,  $M$  is a combination of shear,  $G$ , and osmotic bulk moduli,  $K$ , and is given as  $M = K + 4G/3$ , and  $R$  in turn is defined by the coefficient  $\alpha_n$  in the equation, where  $\alpha_n$  represents the roots of the Bessel functions.

$$R = \frac{1}{4} \left[ 1 + \frac{\alpha_n J_0(\alpha_n)}{J_1(\alpha_n)} \right] \quad (3)$$

where  $J_0$  and  $J_1$  are Bessel functions of the 0th and first orders. In eq. (1),  $\tau_n$  is inversely proportional to the cooperative diffusion coefficient,  $D_c$ , of a gel disc at the surface and is given by the relation<sup>6</sup>

$$\tau_n = \frac{3a^2}{D_c \alpha_n^2} \quad (4)$$

where the diffusion coefficient,  $D_c$ , is given as  $D_c = M/f = (K + 4G/3)/f$ , where  $f$  is the friction coefficient describing the viscous interaction between the polymer and solvent, and  $a$  represents half the disc thickness at the equilibrium state of swelling, which can be experimentally determined.

The series given by eq. (1) is convergent. The first term of the series expansion is dominant at large  $t$ , which correspond to the last stage of the swelling. As is seen from eq. (4),  $\tau_n$  is inversely proportional to the squared of  $\alpha_n$ , where  $\alpha_n$  values are the roots of the Bessel functions. If  $n$  is greater than 1,  $\alpha_n$  increases and  $\tau_n$  decreases rapidly. Therefore, the kinetics of swell-

TABLE I  
Experimentally Measured Parameters

EGDM % $10^{-3}$	1	2	3	4	5	6	7
	5	7.5	10	15	20	25	30
$a_i$ (cm)	0.22	0.25	0.28	0.28	0.28	0.255	0.215
$B_1$	0.67	0.7	0.57	0.49	0.45	0.56	0.48
$\alpha_1$	2.0	1.95	2.2	2.3	2.3	2.2	2.3
$\tau_c$ (min) ( $\langle I \rangle / \langle I_0 \rangle$ )	18	21	24	28	59	72	69
$D_c$ ( $\text{cm}^2 \text{s}^{-1}$ ) $\times 10^{-5}$	1.78	2.2	1.90	1.42	0.64	0.52	0.37
$\tau_c$ (min) ( $\tau_2 / \tau_{02}$ )	22	31	27	29	67	64	62
$D_c$ ( $\text{cm}^2 \text{s}^{-1}$ ) $\times 10^{-5}$ ( $\tau_2 / \tau_{02}$ )	1.45	1.4	1.65	1.4	0.56	0.58	0.415

ing within the limit of large  $t$ , or if the first term of  $\tau_n(\tau_c)$  is much larger than the rest of  $\tau_{nr}$ ,<sup>6</sup> means all high-order terms ( $n \geq 2$ ) in eq. (1) can be dropped such that the swelling and shrinking can be represented by the first-order kinetics.<sup>24</sup> In this case eq. (1) simplifies to

$$\frac{W(t_s)}{W(\infty)} = 1 - B_1 e^{-t_s/\tau_c} \quad (5)$$

and eq. (4) can be given by the following relationship

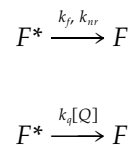
$$\tau_c = \frac{3a^2}{D_c \alpha_1^2} \quad (6)$$

### Fluorescence quenching

The fluorescence and phosphorescence intensities of aromatic molecules are affected by both radiative and nonradiative processes.<sup>25</sup> If the possibility of perturbation from oxygen is excluded, the radiative probabilities are found to be relatively independent of environment and even of molecular species. Environmental effects on nonradiative transitions that are primarily intramolecular in nature are believed to arise from a breakdown of the Born–Oppenheimer approximation.<sup>26</sup> The role of the solvent in such a picture is to add the quasi-continuum of states needed to satisfy energy resonance conditions. The solvent acts as an energy sink for rapid vibrational relaxation that occurs after the rate-limiting transition from the initial state. Years ago Birks et al. studied the influence of solvent viscosity on fluorescence characteristics of pyrene solutions in various solvents and observed that the rate of monomer internal quenching is affected by solvent quality.<sup>27</sup> Weber et al. reported the solvent dependence of energy trapping in phenanthrene block polymers and explained the decrease in fluorescence yield with the static quenching caused by the solvent-induced trapping states.<sup>28</sup> A matrix that changes little with temperature enables the study of molecular properties themselves without changing environmen-

tal influences. Poly(methyl methacrylate) (PMMA) was used as such a matrix in many studies.<sup>29</sup>

Emission of the fluorescence is the radiative transition of an electronically excited molecule from its singlet excited state to its ground state.<sup>30,31</sup> Fluorescence quenching normally refers to any bimolecular process between the excited singlet state of a fluorescence dye and the second species that enhances the decay rate of the excited state. One can schematically represent the process as



where  $F$  and  $F^*$  represent the fluorescent molecule, and its excited form,  $Q$ , is the quencher; and  $k_f$ ,  $k_{nr}$ , and  $k_q$  represent the fluorescence, nonradiative, and quenching rate constants respectively. Many types of processes lead to quenching, as pointed out in the previous paragraph. Kinetically, a quenching process

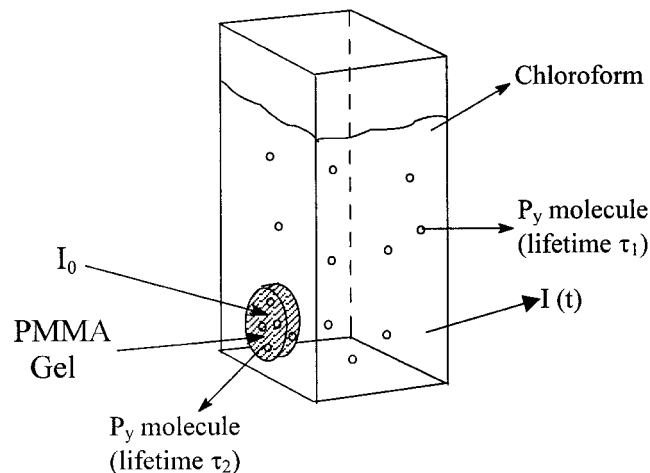
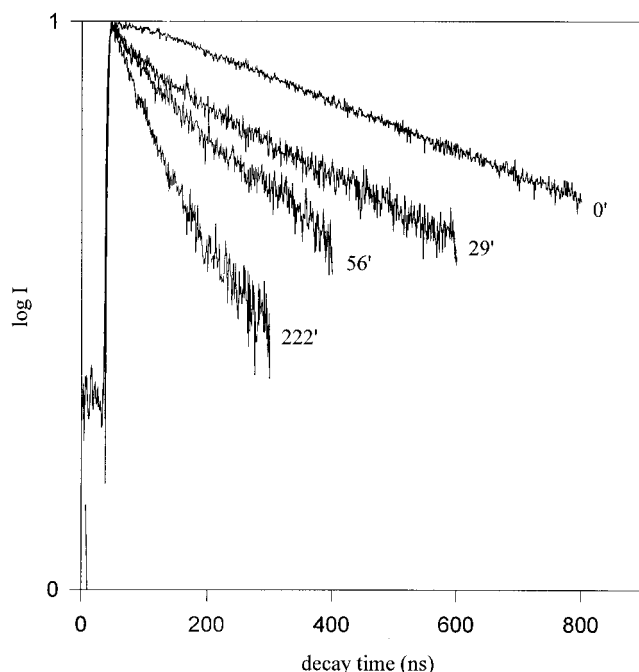


Figure 1 Fluorescence cell in PTI strobe master system during monitoring of gel swelling.  $I_0$  is the excitation and  $I(t)$  the emission intensity at 345 and 395 nm, respectively.



**Figure 2** Log of fluorescence decay profiles,  $I(t)$ , at various swelling steps. The number on each curve present the swelling time,  $t_s$ , in minutes. These experiments were performed according to position described in Figure 1.

can be divided into two main categories: dynamic and static. In dynamic quenching diffusion, forming an encounter pair during the excited state lifetime of the dye leads to quenching. In static quenching diffusion does not occur (which is out of our interest). Dynamic quenching is most likely to occur in fluid solution, where the dye or quencher is free to move. If the quenching rate can be characterized by a single rate coefficient ( $k_q$ ) and the unquenched decay rate of  $F$ , in terms of a unique lifetime,  $\tau_0$ , then the quenching kinetics will follow the Stern–Volmer equation

$$\tau^{-1} = \tau_0^{-1} + k_q[Q] \quad (7)$$

where  $[Q]$  represents the quencher concentration.

## EXPERIMENTAL

EGDM has been commonly used as crosslinker in the synthesis of polymeric networks. The monomers MMA (Merck) and EGDM (Merck, Germany) were freed from the inhibitor by shaking with a 10% aqueous KOH solution, washing with water, and drying over sodium sulfate and were then distilled under reduced pressure over copper chloride.

The FCC of MMA and EGDM was performed in bulk in the presence of 2,2'-azobisisobutyronitrile (AIBN) (0.26 wt %) as an initiator.  $P_y$  was added as a fluorescence probe during the gelation process where  $P_y$  concentration was taken as  $4 \times 10^{-4}M$ . Sample was

deoxygenated by bubbling nitrogen for 10 min, and then radical copolymerization of MMA and EGDM was performed at  $70 \pm 2^\circ C$ . Here, EGDM content was varied from 0.005 to 0.03 vol % for various gel samples, as seen in Table I. After gelation was completed, the gel sample was dried and cut in a disc shape for the swelling experiment. The initial half thicknesses of the gel samples are given in Table I.

FTRF measurements were performed using Photon Technology International's (PTI) strobe master system (SMS). In the strobe, or pulse sampling technique,<sup>31,32</sup> the sample is excited with a pulsed light source. The name comes about because the photo multiplier tube (PMT) is gated or strobed by a voltage pulse that is synchronized with the pulsed light source. The intensity of fluorescence emission is measured in a very narrow time window on each pulse and saved in a computer. The time window is moved after each pulse. The strobe has the effect of turning off the PMT and measuring the emission intensity over a very short time interval window. When the data has been sampled over the appropriate range of time, a decay curve of fluorescence intensity versus time is obtained. Because the strobe technique is intensity-dependent, the strobe instrument is much faster than the SPC and even faster than the phase instrument. The strobe instrument is much easier to use than the SPC, and the data are easier to interpret than those from the phase system. Because of these advantages, SMS is used to monitor the swelling of PMMA gel, which takes about several hours.

Swelling experiments were carried out in the SMS of PTI, employing a pulsed lamp source (0.5 atm of  $N_2$ ). Pyrene molecules were excited at 345 nm and fluorescence decay profiles were obtained at 395 nm during *in situ* swelling experiments, which were performed at room temperature. A disc-shaped gel sample was placed in a 1 cm  $\times$  1 cm quartz cell, where it was attached to one side of a cell by pressing a disc with thick steel wire. The quartz cell was filled with chloroform, and the cell was placed in the SMS system, where fluorescence decay measurements were performed at a  $90^\circ$  angle. The position of the gel in the chloroform-filled fluorescence cell is presented in Figure 1, where lifetimes of  $P_y$  in and out of the gel are shown. When the gel was illuminated by the excitation light,  $I_0$ , the fluorescence decay profiles,  $I(t)$ , are caused by excited  $P_y$  molecules both immersed in the gel and desorbed from the swelling gel. Here it is expected that  $I(t)$  should be composed of the sum of two exponentials with two different lifetimes ( $\tau_1$  and  $\tau_2$ ). The fluorescence decay data were collected over three decades of decay time and fitted by nonlinear least squares using the deconvolution method with a dry gel as a scatterer standard. The uniqueness of the fit of the data to the model is determined by  $\chi^2$  tests ( $\chi^2$

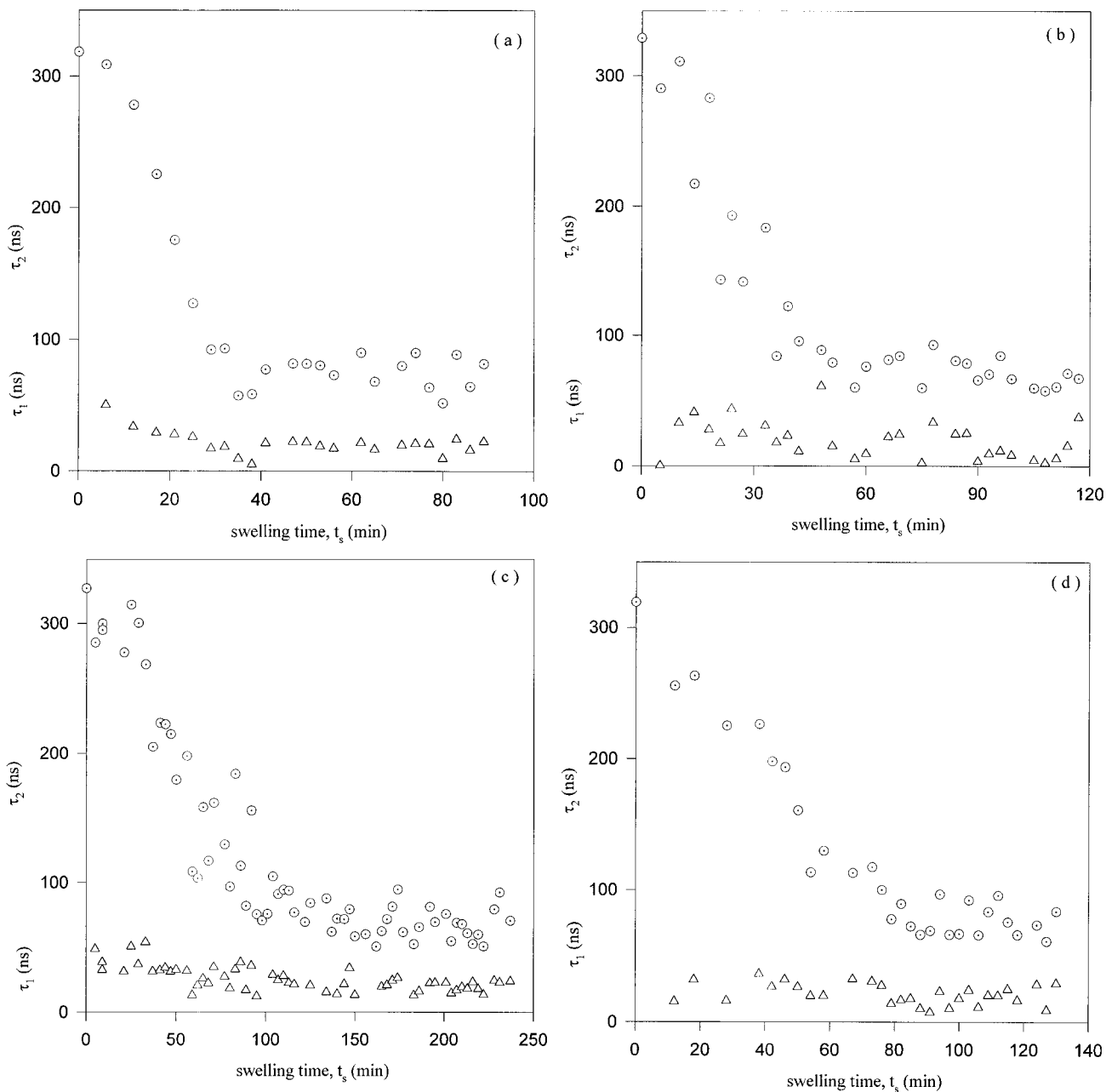


**Figure 3** The plot of the measured  $\tau_2$  and  $\tau_1$  lifetimes versus swelling time,  $t_s$ .  $\tau_1$  and  $\tau_2$  values were obtained by fitting the fluorescence decay profiles to the eq. (8) for the gel samples contained (a) 5 times;  $10^{-3}$ , (b) 15 times;  $10^{-3}$ , (c) 20 times;  $10^{-3}$ , and (d) 25 times;  $10^{-3}$  % EGDM content.

$\leq 1.10$ ), the distribution of the weighted residuals, and the autocorrelation of the residuals.

## RESULTS AND DISCUSSIONS

Decay curves of  $P_y$ , in various swelling times obtained from SMS for gel number 5 in Table I are presented in Figure 2. To probe swelling process during solvent uptake, the fluorescence decay curves were determined and fitted to the sum of two exponentials

$$I(t) = A_1 e^{-t/\tau_1} + A_2 e^{-t/\tau_2} \quad (8)$$

where  $\tau_1$  and  $\tau_2$  are the lifetimes of  $P_y$  outside and inside the gel sample, respectively, and  $A_1$  and  $A_2$  are the corresponding amplitudes of the decay curves. Figure 2 presents the fluorescence decay profiles at various swelling steps (0, 29, 56, and 222 min), where it is seen that as the swelling time,  $t_s$ , increases, excited pyrenes decay faster and faster, which indicates that as solvent uptake,  $W$ , increases, quenching of the excited pyrenes by chloroform increase. In Figure 3(a–d)  $\tau_2$  and  $\tau_1$  lifetimes are plotted versus  $t_s$ , for the gels (1, 4, 5, and 6) swollen in chloroform. It can be seen that  $\tau_2$  values decrease as  $t_s$  increases, however,  $\tau_1$  remains

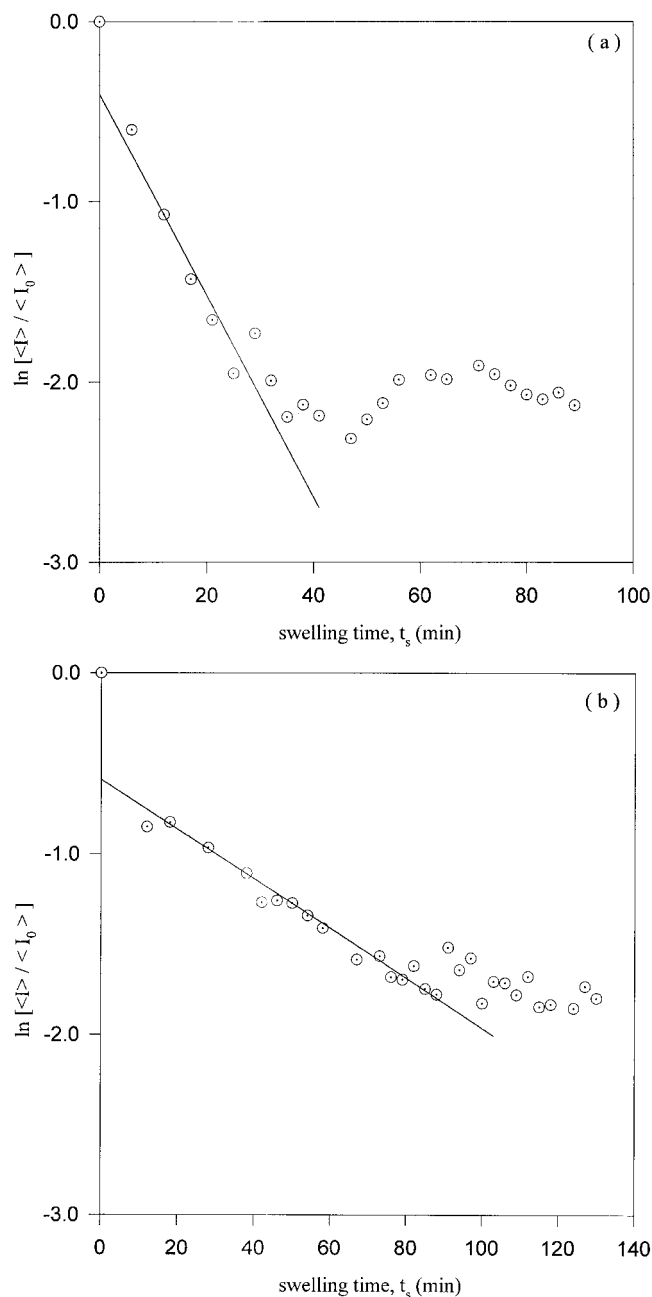


**Figure 4** The plot of  $\langle I \rangle / \langle I_0 \rangle$  versus swelling time,  $t_{sr}$  according to eq. (12) for the gel samples (a) 5 times;  $10^{-3}$  and (b)  $25 \times 10^{-3}$ % EGDM content. The intercept and the slope linear curves produce  $B_1$  and  $\tau_c$  values.

unchanged during swelling. The role of the solvent is to add the quasi-continuum of states needed to satisfy energy resonance conditions, that is, the solvent acts as an energy sink for rapid vibrational relaxation, which occurs after the rate-limiting transition from the initial state. Birks et al. studied the influence of solvent viscosity on the fluorescence characteristics of pyrene solutions in various solvents and observed that the rate of monomer internal quenching is affected by solvent quality.<sup>33</sup>

Because  $\tau_2$  and  $A_2$  values are responsible from the interior of the gel, to quantify the above observation, the area under the fluorescence decay curve is calculated using eq. (8) and the following relationship

$$\langle I \rangle = \int_{t_1}^{t_2} I dt = \tau_2 A_2 \quad (9)$$

where the integral is taking from the peak ( $\tau_1$ ) to the end point ( $\tau_2$ ) of the decay curve. Here  $t_1 = 0$  and  $t_2 = \infty$  are taken to carry out the integration in eq. (9). In fact, the area under the decay curve, that is, the  $\langle I \rangle$  value is equivalent to the steady-state fluorescence intensity. From this analysis we expected to measure  $B_1$  and  $\tau_c$  using the behavior of  $\langle I \rangle$  against swelling time,  $t_{sr}$ . The calculated  $\langle I \rangle$  values decrease as the swelling time,  $t_{sr}$ , is increased, which indicates that the quenching rate of  $P_y$  molecules is increased as chloroform molecules penetrate into the gel. At the beginning, before solvent penetration starts, the  $P_y$  intensity is  $\langle I_0 \rangle$ . When solvent penetration starts, some excited  $P_y$  molecules are quenched and the intensity decreases to  $\langle I \rangle$  at time  $t_{sr}$  where the amount of solvent uptake is  $W$ . Because the  $P_y$  concentration is very low ( $10^{-4}M$ ), it is reasonable to assume that all  $P_y$  molecules are quenched wherever the solvent molecules are entered, that is, the fluorescence intensity change is proportional to solvent uptake. At the equilibrium swelling the  $P_y$  intensity decreased to  $\langle I_\infty \rangle$ , where the solvent uptake by gel is  $W_\infty$ . The relationship between solvent uptake  $W$  and the  $P_y$  intensities,  $\langle I \rangle$ , from the gel

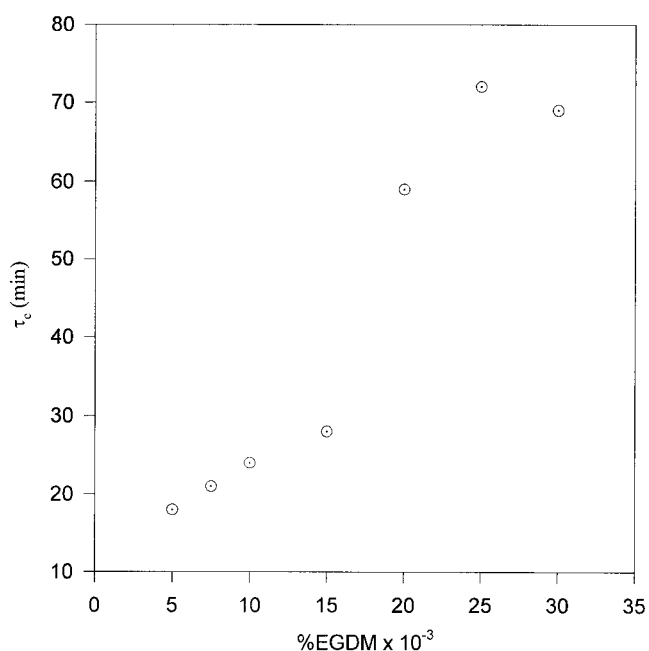


**Figure 5** The plot of the time constant,  $\tau_c$  obtained from eq. (12) versus EGDM content.

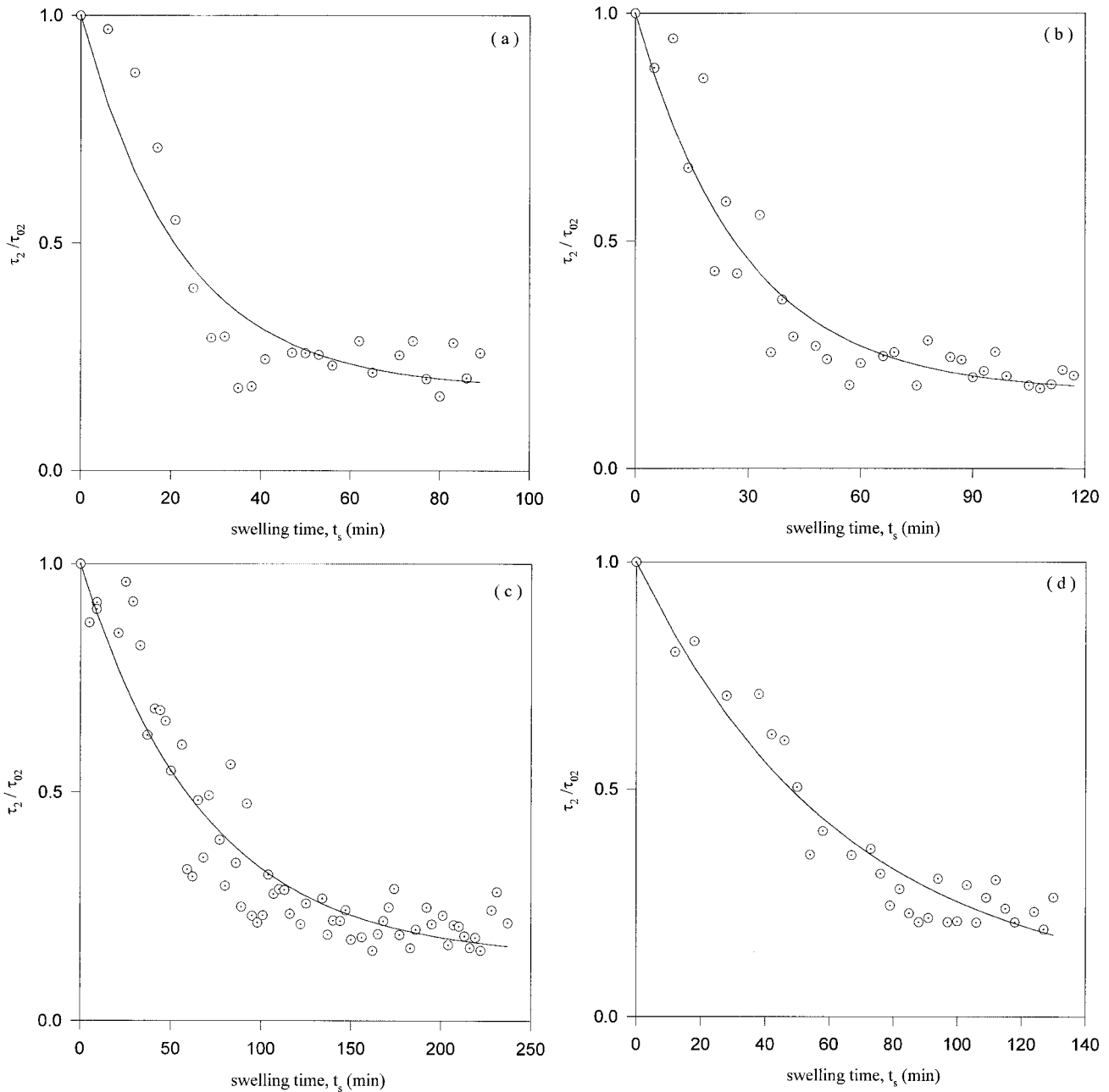


**Figure 6** The plot of the normalized  $\tau_{\square}$  lifetimes versus swelling time,  $t_s$ , for the gel samples contained (a) 5 times;  $10^{-3}$ , (b) 15 times;  $10^{-3}$ , (c) 20 times;  $10^{-3}$ , and (d) 25 times;  $10^{-3}$  % EGDM content. The fit of the data to eq. (15), which produced  $\tau_c$  values, are presented.

during the swelling process are given by the following relation

$$\frac{W}{W_{\infty}} = \frac{\langle I_0 \rangle - \langle I \rangle}{\langle I_0 \rangle - \langle I_{\infty} \rangle} \quad (10)$$

Because  $I_0 \gg I_{\infty}$ , eq. (10) becomes

$$\frac{W}{W_{\infty}} = 1 - \frac{\langle I \rangle}{\langle I_0 \rangle} \quad (11)$$

So eq. (11) predicts that as  $W$  increases,  $\langle I \rangle$  decreases. Combining eq. (11) with eq. (5) and assuming that number of quenched  $P_y$  molecules are proportional to  $W$ , the following relationship is obtained

$$\ln \left[ \frac{\langle I \rangle}{\langle I_0 \rangle} \right] = \ln B_1 - \frac{t_s}{\tau_c} \quad (12)$$

The  $\langle I \rangle$  data are plotted in Figure 4 according to eq. (12) for gel samples of 1 and 6, for which quite linear

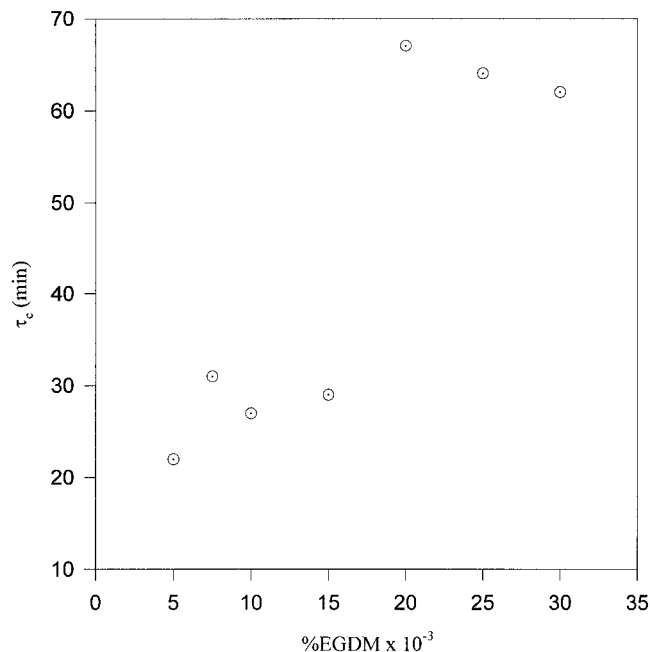


**Figure 7** The plot of the time constant,  $\tau_c$ , obtained from eq. (15) versus EGDM content.

relations are obtained. Linear regression of the curve in Figure 4 yields  $B_1$  and  $\tau_c$  values, which are listed in Table I. Figure 5 presents the plot of  $\tau_c$  versus EGDM content. It can be seen that densely formed (high EGDM content) gels swell more slowly than loosely formed (low EGDM content) gels. Taking into account the dependence of  $B_1$  from  $R$ , eq. (2)  $R$  values can be obtained, and from the  $\alpha_1$ - $R$  dependence,  $\alpha_1$  values produced.<sup>6</sup> Finally, using eq. (6), cooperative diffusion coefficients,  $D_c$ , were determined and are listed in Table I for the gel samples.

To quantify the results in Figure 3 (where exponential decrease in  $\tau_2$  is observed as the swelling time,  $t_s$ , is increased), the Stern-Volmer type of quenching mechanism may be proposed for the fluorescence decay of  $P_y$  in the gel sample. According to Stern-Volmer law  $\tau_2$ , lifetimes can be written as

$$\tau_2^{-1} = \tau_{02}^{-1} + \kappa[W] \quad (13)$$

where  $\tau_{02}$  is the lifetime of  $P_y$  in the dry gel in which no quenching has taken place,  $\kappa$  is the quenching rate constant, and  $[W]$  is the molar solvent concentration in the gel after solvent uptake has started. For low quenching efficiency, where  $\tau_{02}\kappa[W] < 1$ , eq. (13) becomes

$$\tau_2 \approx \tau_{02}(1 - \tau_{02}\kappa[W]) \quad (14)$$

If eq. (14) is integrated over the differential volume,  $dv$ , of the gel from initial to final thicknesses of the gel, the following relationship is obtained.

$$\frac{\tau_2}{\tau_{02}} = 1 - C + CB_1e^{-t_s/\tau_c} \quad (15)$$

where  $C = \tau_{02}\kappa W_\infty/v$  and  $v$  is the swollen volume of the gel. Then eq. (15) was fitted to the data of normalized mean lifetimes of  $P_y$  in Figure 6 for the gel samples of 1, 4, 5, and 6. The  $\tau_c$  values were obtained from the curves in Figure 6. Using known  $B_1$  values from previous calculations,  $\tau_c$  values were obtained and are listed in Table I. The  $\tau_c$  values obtained using eq. (15) are plotted versus EGDM content in Figure 7, where

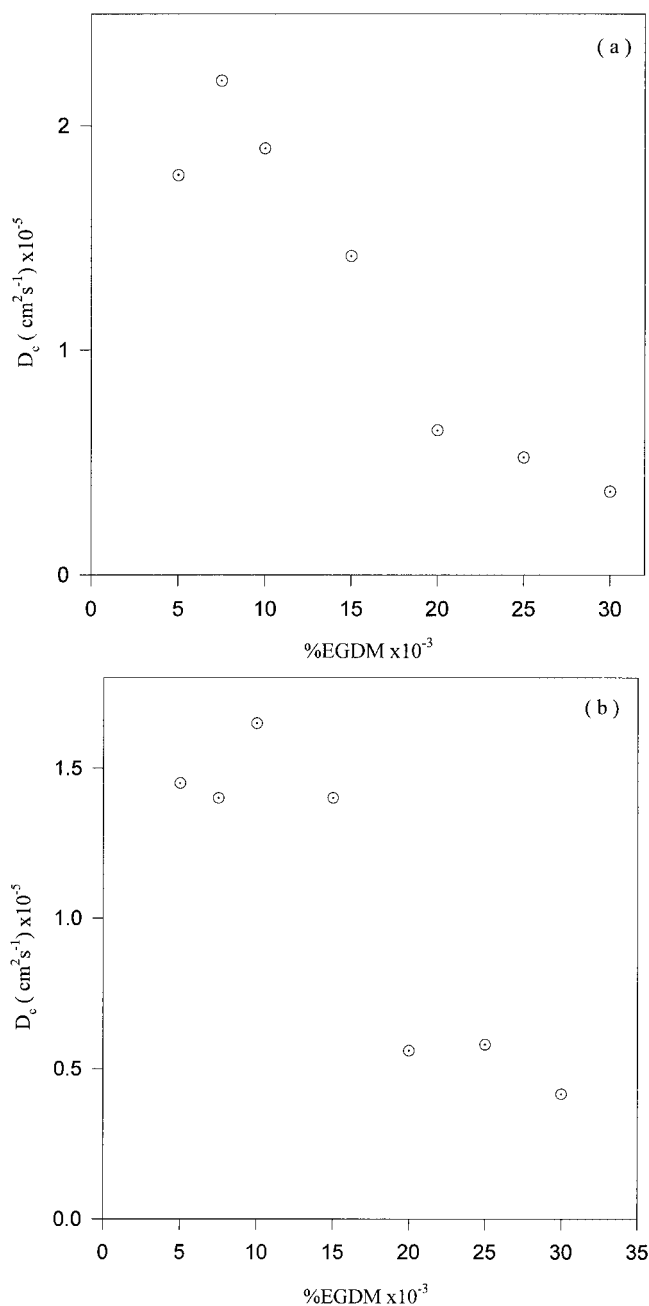


**Figure 8** The plot of cooperative diffusion coefficient,  $D_c$ , versus EGDM content from the analysis of (a) eq. (12) and (b) eq. (15).



similar behavior is observed with the  $\tau_c$  values obtained from eq. (12). In other words, densely formed gels swell slower than loosely formed gels.

Cooperative diffusion coefficients,  $D_c$ , were calculated from  $\tau_c$  values obtained from eq. (15) and are listed in Table I. The  $D_c$  values obtained from two preceding analyses are plotted versus EGDM content in Figure 8. In both cases  $D_c$  values decreased as EGDM content increased. The gel segment moves much faster in loosely formed gels than in densely formed gels.

In conclusion, this article presents the FTRF technique to be used to measure cooperative diffusion coefficients during the swelling of a polymeric gel. It can be argued that measuring lifetimes by using FTRF in a swelling gel provides data that can be used without correction. However, data obtained by using the steady-state fluorescence method need quite a bit of correction in intensity because of certain effects. The different  $D_c$  values listed in Table I most probably came from the differences in lifetime and intensity measurements.

## References

1. Tanaka, T.; Filmore, D. *Chem Phys* 1979, 70, 1214.
2. Peters, A.; Candau, S. J. *Macromolecules* 1986, 19, 1952.
3. Chiarelli, P.; De Rossi, D. *Prog Colloid Polym Sci* 1988, 7, 44.
4. Dusek, K.; Prins, W. *Adv Polym Sci* 1969, 6, 1.
5. Candau, S.; Baltide, J.; Delsanti, M. *Adv Polym Sci* 1982, 7, 44.
6. Li, Y.; Tanaka, T. *J Chem Phys* 1990, 92, 1365.
7. Pekcan, Ö.; Winnik, M. A.; Egan, L. S.; Croucher, M. D. *Macromolecules* 1983, 16, 669.
8. Pekcan, Ö.; Winnik, M. A.; Croucher, M. D. *Phys Rev Lett* 1988, 61, 641.
9. Pekcan, Ö. *Chem Phys Lett* 1992, 20, 198.
10. Pekcan, Ö. *Trends Polym Sci* 1994, 2, 236.
11. Pekcan, Ö. *Chem Phys* 1993, 177, 619.
12. Pekcan, Ö.; Winnik, M. A.; Croucher, M. D. *Macromolecules* 1990, 23, 2673.
13. Wang, Y.; Winnik, M. A. *Macromolecules* 1993, 26, 3147.
14. Pekcan, Ö. *J Appl Polym Sci* 1993, 49, 151.
15. Pekcan, Ö. *J Appl Polym Sci* 1996, 59, 521.
16. Peters, A.; Candau, S. J. *Macromolecules* 1998, 21, 2278.
17. Bastide, J.; Duoplessix, R.; Picot, C.; Candau, S. *Macromolecules* 1984, 17, 83.
18. Wu, C.; Yan, C. Y. *Macromolecules* 1994, 27, 4516.
19. Panxviel, J. C.; Dunn, B.; Zink, J. J. *J Phys Chem* 1989, 93, 2134.
20. Pekcan, Ö.; Yilmaz, Y.; Okay, O. *Chem Phys Lett* 1994, 229, 537.
21. Pekcan, Ö.; Yilmaz, Y.; Okay, O. *Polymer* 1996, 37, 2049.
22. Yilmaz, Y.; Pekcan, Ö. *Polymer* 1998, 39, 5351.
23. Erdoğan, M.; Pekcan, Ö. *J Polym Sci Part B* 2000, 38, 739.
24. Tanaka, T. *Phys Rev Lett* 1980, 45, 1636.
25. Kropp, L. J.; Dawson, R. W. In *International Conference on Molecular Luminescence*; Lim, E. C., Ed.; W. A. Benjamin: New York, 1969.
26. Bixon, M.; Jortner, J. *J Chem Phys* 1968, 48, 715.
27. Birks, J. B.; Lumb, M. D.; Munro, I. H. *Proc Roy Soc A* 1964, 277, 289.
28. Kamioka, K.; Weber, S. E.; Morishima, Y. *Macromolecules* 1988, 21, 972.
29. Jones, P. F.; Siegel, J. *J Chem Phys* 1964, 50, 1134.
30. Birks, J. B. *Photophysics of Aromatic Molecule*; Wiley-Interscience: New York, 1971.
31. Lakowicz, J. R. *Principles of Fluorescence Spectroscopy*; Plenum Press: New York, 1983.
32. Ware, W. R.; James, D. R.; Siemianczuk, A. *Rev Sci Inst* 1992, 63, 1710.
33. Birks, J. B.; Lumb, M. D.; Mumra, J. H. *Proc. R Soc Sev A* 1989, 277, 289.